CHAPTER 5.

The Role of Lysine Acetylation in Regulating Cardiac Fatty Acid β-Oxidation and Hypertrophy

My role in this work involved performing all experiments (except those noted below), as well as the writing of the manuscript. Cory Wagg perfused the mouse heart, and Sowndramalingam Sankaralingam performed perfusion data analysis. Donna Becker performed the echocardiography for in vivo cardiac functions.

Manuscript Status: This manuscript is in preparation for submission as an original article.

CHAPTER 5.

The Role of Lysine Acetylation in Regulating Cardiac Fatty Acid β-Oxidation and Hypertrophy

Abstract

Aims: Lysine acetylation has emerged as a novel post-translational pathway that regulates the activities of enzymes involved in fatty acid β-oxidation and hypertrophy. We examined whether lysine acetylation controls heart fatty acid β-oxidation and mediators of hypertrophy in pressure overload-induced heart failure.

Methods and results: C57Bl/6J mice (4-wk of age) were subjected to a high fat diet (HFD, 60% kcal from fat) to induce obesity. Heart failure was induced by abdominal aortic constriction (AAC). At 4 wk post-AAC, mice were either switched to a low-fat diet (LFD, 4% kcal from fat; HF AAC LF) or maintained on a HFD (HF AAC HF) for a further 10 wk period. After 18 weeks, HF AAC HF mice weighed significantly more than HF AAC LF mice. Cardiac hypertrophy evident in HF AAC HF mice was associated with SIRT1 mediated inhibition of FoxO1 while activation of FoxO1 and AMPK blunted this effect in HF AAC LF mice. In isolated working hearts, insulin stimulated glucose oxidation rates were also significantly increased in HF AAC LF hearts, compared to HF AAC HF hearts. Activity of the fatty acid β-oxidation enzyme, long chain acyl CoA dehydrogenase (LCAD) was

significantly increased in hearts from HF AAC HF vs HF AAC LF mice, and was associated with LCAD hyperacetylation. Heart failure observed *in vivo* by echocardiography in HF AAC HF was significantly improved in HF AAC LF mice.

Conclusions: We conclude that increased LCAD and FoxO1 acetylation enhances cardiac fatty acid β-oxidation and reduces hypertrophy, respectively.

5.1 INTRODUCTION

Obesity is widely recognized as a risk factor for heart failure (257,258). Obesity is associated with left ventricular hypertrophy and dilatation, features that are known to precede the development of overt heart failure (259,260). For every increase in body mass index (BMI) by 1 the risk of heart failure increases by 5% in men and 7% in women (261). Compared with lean subjects, overweight and obese individuals had a 49% and 180% increased risk of heart failure respectively (262).

One major pathway that is altered in both obesity and heart failure is cardiac energy metabolism (1,89). Insulin resistance states such as obesity and diabetes are associated with dramatic changes in cardiac energy metabolism, which include an increase in fatty acid β-oxidation, and a decrease in glucose oxidation (58,61,89). We previously showed that mice fed a high fat diet developed cardiac insulin resistance that was accompanied by increased cardiac fatty acid β-oxidation and decreased glucose oxidation (61). Similarly *ob/ob* and *db/db* mice that exhibit insulin resistance and obesity have increased cardiac fatty acid β-oxidation and reduced cardiac efficiency (58). Obesity itself markedly decreases glucose oxidation. In obese women, both myocardial fatty acid uptake and oxidation are increased and directly correlate with the degree of insulin resistance (91). Thus obesity and the associated insulin resistance

adversely affect cardiac metabolism and function. Heart failure even in the absence of risk factors such as obesity can also lead to dramatic alterations in cardiac energy metabolism (1). A decrease in energy production and or a decrease in energy efficiency can result in a state of "energetic deficit" in the heart (129,137,263). Using various experimental models of heart failure, we have shown that a decrease in insulin-stimulated glucose oxidation precedes heart failure and that stimulating glucose oxidation can improve both cardiac efficiency and function (59,137,138,264).

Non-histone lysine acetylation is suggested as an important post-translational modification which can regulate cardiac energy metabolism (18-21). Key enzymes of glycolysis, glucose oxidation, fatty acid β-oxidation, and tricarboxylic cycle are acetylated at least on one lysine residue (159,194,191,200). Furthermore, proteins involved in cardiac hypertrophy such as FoxO1 have been shown to be under acetylation control (187,188). However, the impact of this post-translational modification on the activity of key enzymes involved in fatty acid metabolism and hypertrophy is poorly defined. In mitochondria, general control of amino acid synthesis 5 like 1(GCN5L1) is recently characterized as an acetyltransferase which plays important role metabolism (211). Protein deacetylation is mediated by a family of seven enzymes called sirtuins (SIRT1-7) (159,191,194). SIRT3 is suggested as a major mitochondrial deacetylase which controls the activity of key enzymes

involved in glucose and fatty acid β-oxidation (191,194,200). The impact of lysine acetylation on fatty acid β-oxidation in the setting of heart failure has never been addressed before. In addition, SIRT1 plays an important role in cardiac hypertrophy (228,236). The transcriptional factor FoxO1 which play a key role in regulation of cardiomyocyte proliferation and cardiac hypertrophy is a target for SIRT1 deacetylation (187,188). SIRT1 can deacetylate and repress FoxO1 activity (187,188). The purpose of this study is to determine the role of lysine acetylation in regulation of cardiac energy metabolism and the contribution of this post-translational modification to the development of cardiac hypertrophy.

5.2 MATERIALS AND METHODS

Mice received care and were treated according to the guidelines of the Canadian Council on Animal Care, and all procedures performed on animals were approved by the University of Alberta Health Sciences Animal Welfare Committee. GTT and echocardiography were conducted to determine levels of blood glucose and *in vivo* cardiac function, respectively. Hearts isolated from pentobarbital euthanized mice were perfused as isolated working hearts with Krebs-Henseleit solution containing 2.5 mM Ca^{2+}, 5 mM [U-^{14}C]glucose, 0.8 mM [9,10-^{3}H]palmitate prebound to 3% albumin, in the presence or absence of 100 μU/mL insulin, as described in details in **chapter 2**. At the end of the perfusion, hearts were immediately frozen in liquid N_2 and processed for acetylation status. Protocols for assessment of LCAD activity, immunoprecipitation, immunoblotting, and statistical analysis are described in details in **chapter 2** of this thesis.

5.3 RESULTS

5.3.1 Body weight and glucose tolerance:

After 8 weeks mice (4-wk of age) fed the standard chow (Low Fat Diet, LFD) weighed 26.1±1.2 g (Figure 5-1A). HFD fed mice weighed significantly more than LFD fed mice (34.8±2.0 g, $P<0.05$). HF AAC HF and HF AAC LF mice had similar body weights after 8 weeks of HFD (35.7±1.4 vs. 36.0±2.2 g). Although mice were randomly assigned to the HF AAC LF sub-group after 8 weeks from the HF AAC group, data from this subgroup of mice are presented separately at 8 weeks to demonstrate that the parameters are similar at 8 weeks before being switched to LFD. In our study this process of randomization has removed any selection bias. After 18 weeks HFD fed mice had a significantly higher body weight compared to LFD fed mice (48.3±1.5 vs. 31.2±1.2 g, $P<0.001$). Interestingly, HF AAC mice switched to LFD (HF AAC LF) after 8 weeks, did not lose but maintained their body weight and was significantly lower compared to HF AAC HF mice (43.5±1.9 vs. 35.1±1.6 g, $P<0.01$).

To analyze the response of mice to a glucose challenge, we performed oral GTT after 8 weeks to confirm the development of impaired glucose tolerance in these mice before switching the diet. After 8 weeks of feeding protocol, the area under the curve (AUC) was significantly higher in all groups of HFD compared to LFD fed mice (Figure 5-1B). The AUC for HFD (56.9±2.6 mmol/l.min), HF AAC HF (58.6±2.1), HF AAC LF

(60.1±2.7 mmol/l.min) was higher compared to LFD fed mice (46.1±1.2 mmol/l.min, P<0.05).

After 18 weeks, HFD fed mice had sustained impaired glucose tolerance (Figure 5-1B). The AUC for HFD fed and HF AAC HF mice (68.7±2.6 and 69.1±3.2 mmol/l.min) was significantly higher (P<0.01) than that of LFD fed mice (44.5±1.4 mmol/l.min). There was a dramatic improvement in glucose tolerance in HF AAC mice switched to LFD. The AUC in the HF AAC LF group was 49.1±1.0 mmol/l.min and was not different from LFD fed mice.

5.3.2 In vivo (echocardiography) analyses of cardiac function:

LFD fed sham mice had normal diastolic and systolic function. AAC induced a diastolic dysfunction in HFD fed mice as early as 2 weeks after the procedure as assessed by an increased E/A ratio (HF AAC; 1.9±0.1vs. 1.5±0.04, p<0.05) compared to baseline (Figure 5-2A). Switching to LFD improves diastolic function as shown by a decrease in E/A ratio 1.6±0.05, P<0.05 that was evident after 18 weeks. Mitral tissue doppler E'/A' ratio and E/E' ratio (marker of left atrial filling pressure) were also measured as markers of diastolic function (Figure 5-2B). Decrease in E'/A' ratio and an increase in E/E' ratio represent diastolic dysfunction. Significant changes in these parameters are noted as early as 2 weeks post-AAC compared to baseline suggesting diastolic dysfunction in HF AAC HF mice. Being more sensitive markers of diastolic function, improvements in E'/A' ratio and

E/E' ratio were observed as early as 6 weeks after switching the HF AAC mice to a LFD even before significant changes in E/A ratio was observed (Figure 5-2C). Systolic function measured as percent ejection fraction was normal in LFD fed sham and HFD fed sham mice (54.8±4.4 and 57.7±3.1%) (Figure 5-2D). AAC induced a small but significant reduction in ejection fraction (45.3±2.3%) compared to baseline (55.3±2.5%, $P<0.05$) in HFD fed mice (Figure 5-2D). Switching to LFD also improved systolic function (51.2±1.6%).

5.3.3 Mechanisms of cardiac hypertrophy in obese heart failure mice:

AAC induced a modest level of cardiac hypertrophy in HFD fed mice compared to LFD and HFD fed sham mice (LV mass, 149.2±5.7 vs. 93.7±2.0 and 117.7±5.5 mg, $P<0.01$) (Figure 5-3A). Switching HF AAC mice to LFD resulted in significantly lower LV mass (122.0±2.9, $P<0.01$). It is important to note that both HF AAC HF and HF AAC LF mice had similar LV mass after 8 weeks. While hearts from both groups of mice continued to hypertrophy, the rate of hypertrophy was blunted in the HF AAC LF mice, and was significant as early as 14 weeks. Hypertrophy assessed by echocardiography was confirmed by measuring heart weights after 18 weeks (Figure 5-3B). We wanted to understand the mechanisms involved in cardiac hypertrophy in HF AAC HF hearts. When compared to HFD fed sham mice, a 2.5-fold increase in SIRT1 expression (Figure 5-3C) was observed that was accompanied by a 50% reduction in

abundance of acetylated FoxO1 (Ac-FoxO1) (inhibition) in hearts from HF AAC HF mice (Figure 5-3D). Inhibition of FoxO1 was accompanied by decrease in downstream atrogin-1, a mediator of muscle atrophy (Figure 5-3E). On the other hand, a decrease in SIRT1 and an increase in acetylation (activation) of FoxO1 were associated with increased atrogin-1 expression which played a role in decreased LV mass and a blunted rate of cardiac hypertrophy observed in HF AAC LF hearts. Activation (phosphorylation) of P38MAPK accompanied the activation of AMPK and has been suggested to increase atrogin-1 expression observed in our study (Figure 5-3F).

In addition to SIRT1, a dramatic increase in PKC-α also contributes to cardiac hypertrophy in HF AAC HF hearts (Figure 5-4A). This could subsequently result in activation (increased phosphorylation) of mTOR and P70S6K ultimately resulting in increased protein synthesis and cardiac hypertrophy in HF AAC HF hearts (Figure 5-4B&C). The decrease in LV mass observed in HF AAC LF was also associated with activation (increased phosphorylation) of AMPK (Figure 5-4D).

5.3.4 Cardiac energy metabolism and insulin resistance:

Insulin stimulated a 2-fold increase in cardiac glucose oxidation in the LFD fed mice (Figure 5-5A). This response was blunted in both HFD fed sham and HF AAC HF mice suggesting insulin resistance. Interestingly, switching to LFD completely reversed insulin resistance that

resulted in a dramatic 3-fold increase in glucose oxidation in the HF AAC LF hearts. In HF AAC LF hearts, the insulin stimulated glucose oxidation was significantly higher than HF AAC HF hearts even after normalizing to cardiac work. Further, in response to insulin, LFD fed sham mice had a significant decrease in cardiac palmitate oxidation (Figure 5-5B) an effect that was blunted in HF AAC HF hearts but reversed in HF AAC LF hearts. In summary, in HF AAC HF hearts with diastolic dysfunction insulin resistance and greater reliance on palmitate oxidation are observed. In contrast, HF AAC LF hearts with improved diastolic function are insulin sensitive and rely heavily on glucose oxidation.

5.3.5 Acetylation control of cardiac metabolic enzymes:

Acetylation as a post-translational modification has gained considerable interest in the regulation of energy metabolism. HFD stimulated a 2-fold increase in GCN5L1 expression compared to LFD fed sham mice and was further increased in the HF AAC HF hearts (Figure 5-6A). HF AAC LF hearts had significantly lower GCN5L1 expression compared to HF AAC HF hearts. However, we did not find changes in SIRT3 expression (Figure 5-6B). Parallel to increased abundance of GCN5L1, acetylation of LCAD was increased in HFD fed sham and HF AAC HF mice (Figure 5-6C). Interestingly, HF AAC LF mice had decreased acetylation of LCAD. LCAD activity increased in parallel to LCAD acetylation (Figure 5-6D). We further show a positive correlation

between abundance of acetylated LCAD and palmitate oxidation rates suggesting that acetylation of LCAD could activate LCAD and therefore stimulate fatty acid β-oxidation in these hearts (Figure 5-6E).

5.3.6 Insulin signaling in failing hearts:

Phosphorylation of Akt was markedly enhanced in obese-heart failure mice switched to LFD (Figure 5-7A). Hearts from HFD fed sham and HF AAC HF mice are insulin resistant as shown by decreased abundance of phosphorylation of GSK-3β (Figure 5-7B). Switching to LFD resulted in enhanced insulin signaling as shown by increased P-Akt and P-GSK3β expression in HF AAC LF group.

Figure 5-1: Total body weight and glucose tolerance for LFD and HFD fed mice.

A) Feeding high fat diet for 18 weeks increases body weight in both HFD fed sham mice and HF AAC HF groups compared to mice fed low fat diet (LFD). Switching HF AAC mice to LFD lowers body weight. **B)** High fat feeding for 18 weeks impairs oral glucose tolerance in mice fed a high fat diet (HFD fed sham and HF AAC HF) in comparison to LFD fed mice. Switching HF AAC mice to LFD dramatically improves glucose tolerance. ** $P<0.01$, *** $P<0.001$ vs. LF Sham; † $P<0.05$ vs. HF AAC HF, †† $P<0.01$ vs. HF AAC HF. Values represent mean ± SEM (n=6).

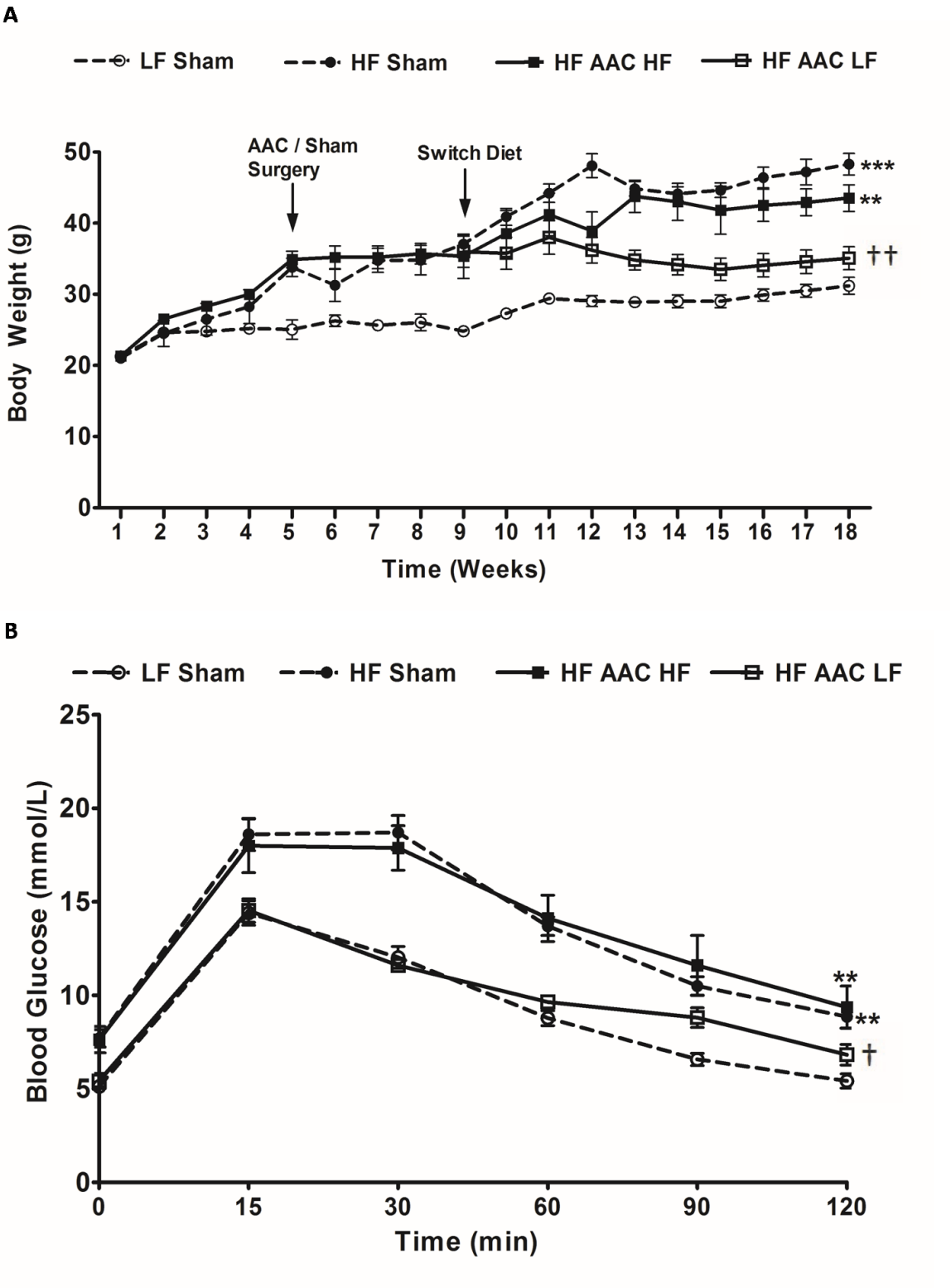
A
LF Sham
HF Sham
HF AAC HF
HF AAC LF
AAC / Sham Surgery
Switch Diet
Body Weight (g)
Time (Weeks)
***
**
††
B
LF Sham
HF Sham
HF AAC HF
HF AAC LF
Blood Glucose (mmol/L)
Time (min)
**
**
†

Figure 5-1

Figure 5-2: In vivo cardiac function as assessed by echocardiography.

A) HF AAC HF mice developed diastolic dysfunction as measured by an increase in E/A ratio that improved when switched to LFD. **B)** HF AAC mice developed diastolic dysfunction as seen by a decrease in E'/A' ratio and the improvement in function in HF AAC LF mice is seen as early as 14 weeks. **C)** HF AAC HF mice developed diastolic dysfunction as seen by an increase in E/E' ratio and the improvement in function in HF AAC LF mice are seen as early as 14 weeks. **D)** Systolic dysfunction in HF AAC HF mice was observed after 14 weeks and improved upon switching to LFD.
† $P<0.05$ vs. HF AAC HF at the same time point. * $P<0.05$, ** $P<0.01$ vs. baseline; Values represent mean ± SEM (n=6).

A

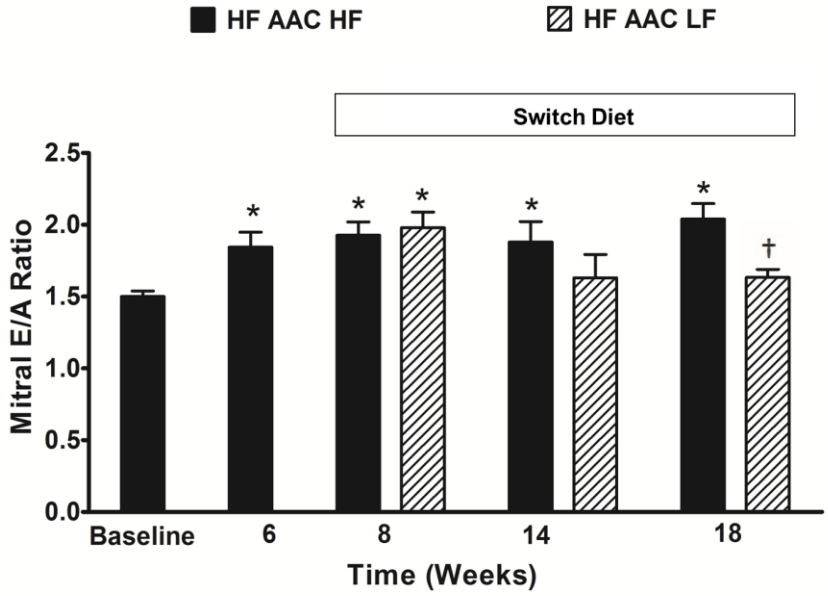
HF AAC HF
HF AAC LF
Switch Diet
Mitral E/A Ratio
2.5
2.0
1.5
1.0
0.5
0.0
Baseline
6
8
14
18
Time (Weeks)

B

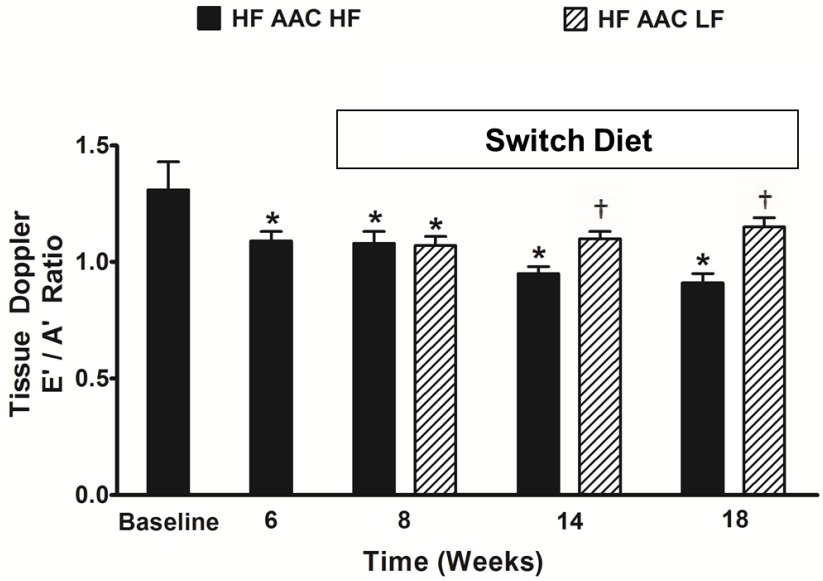
HF AAC HF
HF AAC LF
Switch Diet
Tissue Doppler
E' / A' Ratio
1.5
1.0
0.5
0.0
Baseline
6
8
14
18
Time (Weeks)

Figure 5-2

C

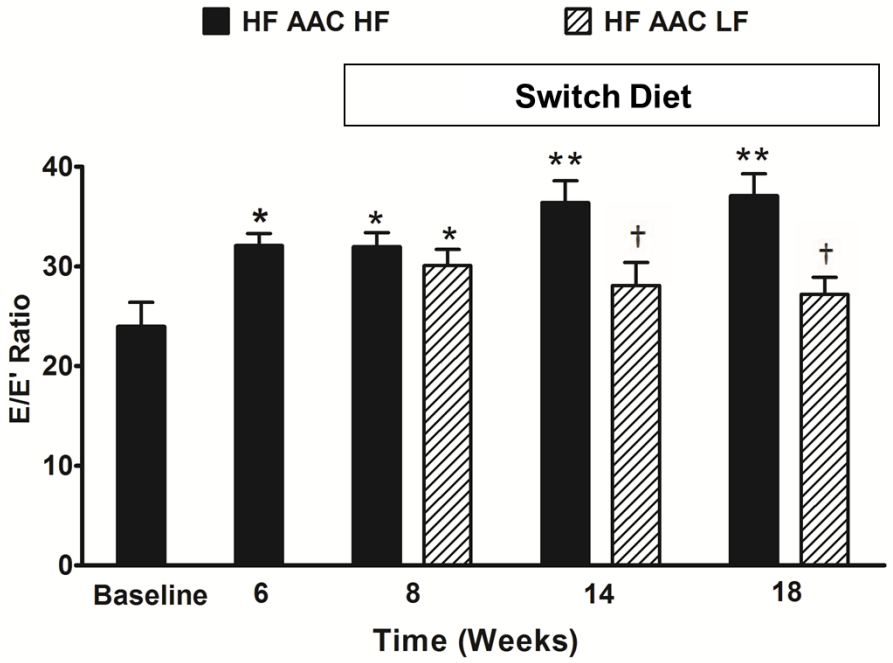
HF AAC HF
HF AAC LF
Switch Diet
E/E' Ratio
40
30
20
10
0
*
*
*
**
†
**
†
Baseline
6
8
14
18
Time (Weeks)

D

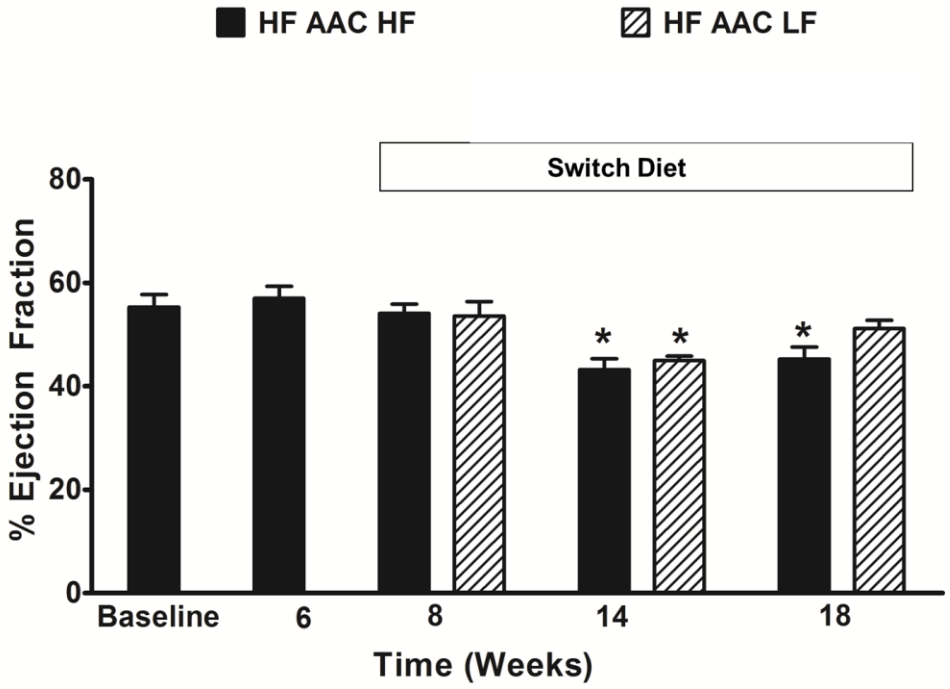
HF AAC HF
HF AAC LF
Switch Diet
% Ejection Fraction
80
60
40
20
0
*
*
*
Baseline
6
8
14
18
Time (Weeks)

Figure 5-2

Figure 5-3: Mechanisms of cardiac hypertrophy in mice fed a low or high fat diet.

A) Cardiac hypertrophy as measured by an increase in LV mass developed in the HF AAC HF mice that was blunted in the HF AAC LF mice. **B)** The increase in left ventricular mass in HF AAC HF compared to LFD fed sham mice partially resolved on switching to LFD. **C)** HFD decreased while HF AAC HF increased SIRT1 expression in comparison to LFD fed sham mice, an effect that was reversed upon switching obese-heart failure mice to LFD. **D)** In parallel to SIRT1 expression, acetylated (Ac) FoxO1 increased in HFD fed sham mice while the abundance decreased in HF AAC HF. Upon switching to LFD, HF AAC LF mice had increased acetylated (activated) FoxO1. **E)** Atrogin-1 expression was significantly decreased in the HF AAC HF mice, while the expression was increased in HF AAC LF mice. **F)** An increase in P-P38MAPK was observed in HF AAC LF mice in comparison to HF AAC HF mice.

* $P<0.05$ vs. baseline or LF Sham; † $P<0.05$ vs. HF AAC HF; †† $P<0.01$ vs. HF Sham or HF AAC HF (as appropriate); ‡ $P<0.05$ vs. HF AAC HF. Values represent mean ± SEM (n=6).

A

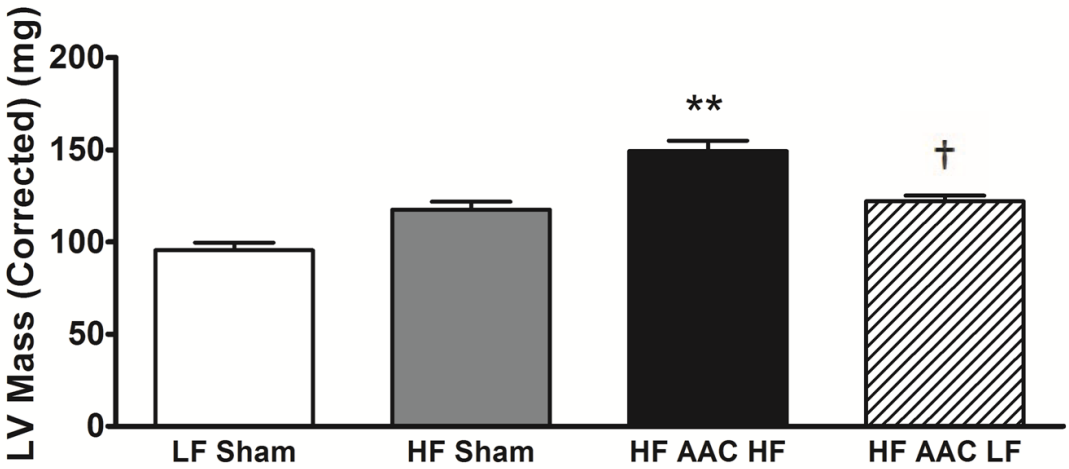
LV Mass (Corrected) (mg)
200
150
100
50
0
**
†
LF Sham
HF Sham
HF AAC HF
HF AAC LF

B

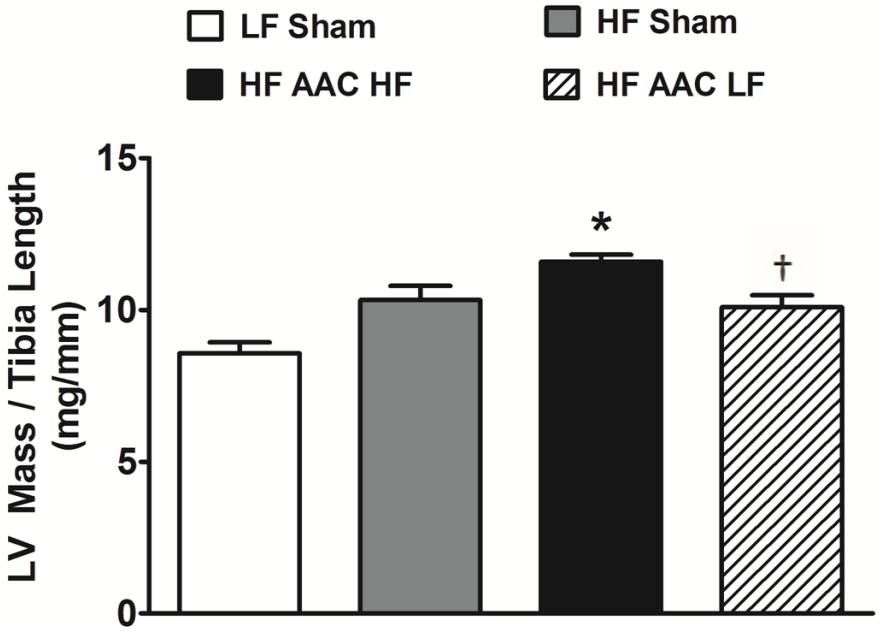
LF Sham
HF Sham
HF AAC HF
HF AAC LF
LV Mass / Tibia Length (mg/mm)
15
10
5
0
*
†

Figure 5-3

C

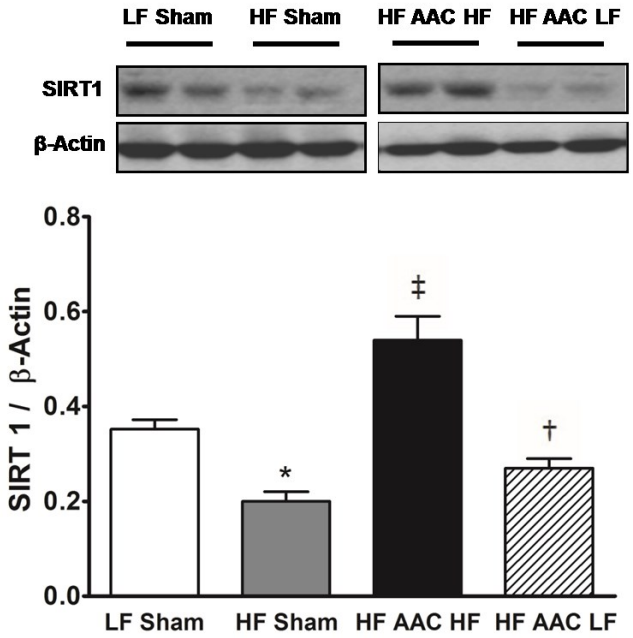
LF Sham
HF Sham
HF AAC HF
HF AAC LF
SIRT1
β-Actin
SIRT 1 / β-Actin
0.8
0.6
0.4
0.2
0.0
*
‡
†
LF Sham
HF Sham
HF AAC HF
HF AAC LF

D

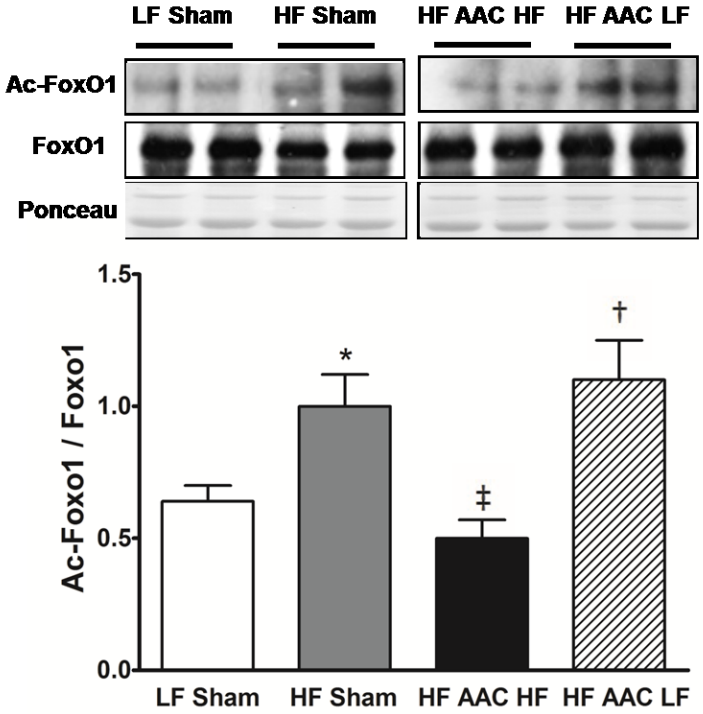
LF Sham
HF Sham
HF AAC HF
HF AAC LF
Ac-FoxO1
FoxO1
Ponceau
Ac-Foxo1 / Foxo1
1.5
1.0
0.5
0.0
*
‡
†
LF Sham
HF Sham
HF AAC HF
HF AAC LF

Figure 5-3

E

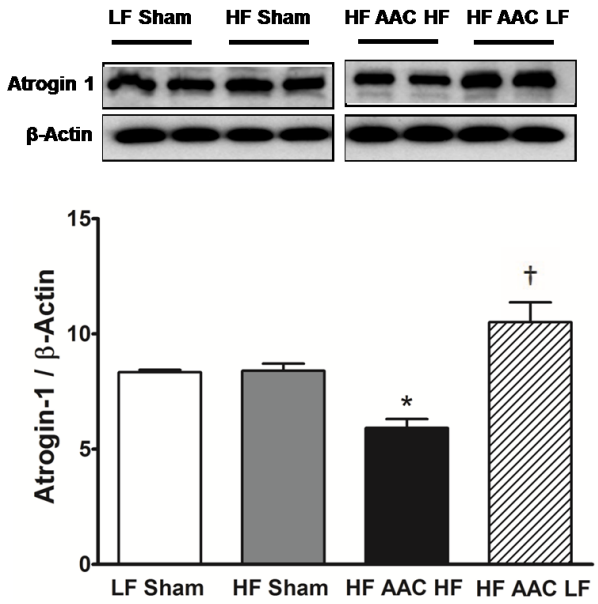
LF Sham
HF Sham
HF AAC HF
HF AAC LF
Atrogin 1
β-Actin
Atrogin-1 / β-Actin
15
10
5
0
*
†
LF Sham
HF Sham
HF AAC HF
HF AAC LF

F

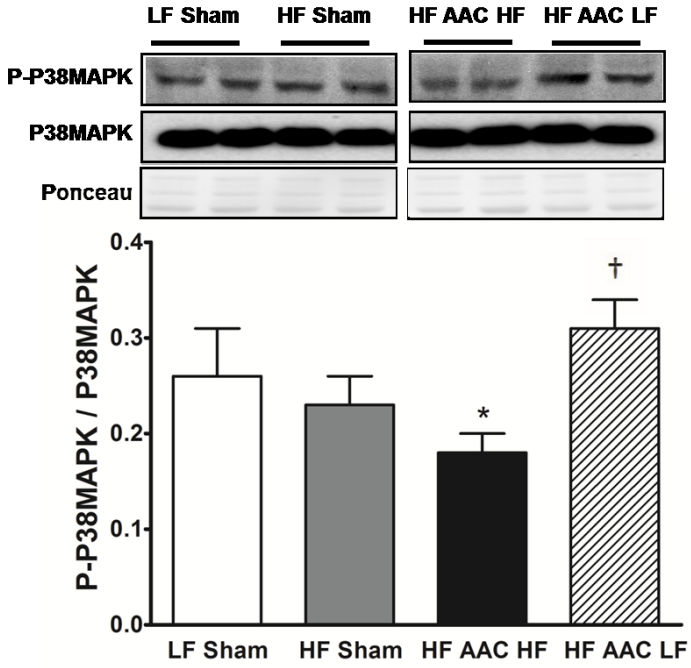
LF Sham
HF Sham
HF AAC HF
HF AAC LF
P-P38MAPK
P38MAPK
Ponceau
P-P38MAPK / P38MAPK
0.4
0.3
0.2
0.1
0.0
*
†
LF Sham
HF Sham
HF AAC HF
HF AAC LF

Figure 5-3

Figure 5-4: Contribution of PKC-α-mTOR pathway to cardiac hypertrophy in LFD and HFD fed mice.

A) Dramatic increase in PKC-α is observed in HF AAC HF that is markedly blunted in HF AAC LF. **B)** P-mTOR is increased in HF AAC HF mice. Switching to low fat diet reverses this effect. **C)** The increased P-P70S6K expression in HF AAC HF mice was reversed by switching to low fat diet. **D)** High fat feeding did not affect AMPK. However, phosphorylation of AMPK is increased in HF AAC HF mice switched to low fat diet.

* $P<0.05$, *** $P<0.001$ vs. LF Sham; † $P<0.05$, †† $P<0.01$ vs. HF AAC HF. Values represent mean ± SEM (n=5-6).

A

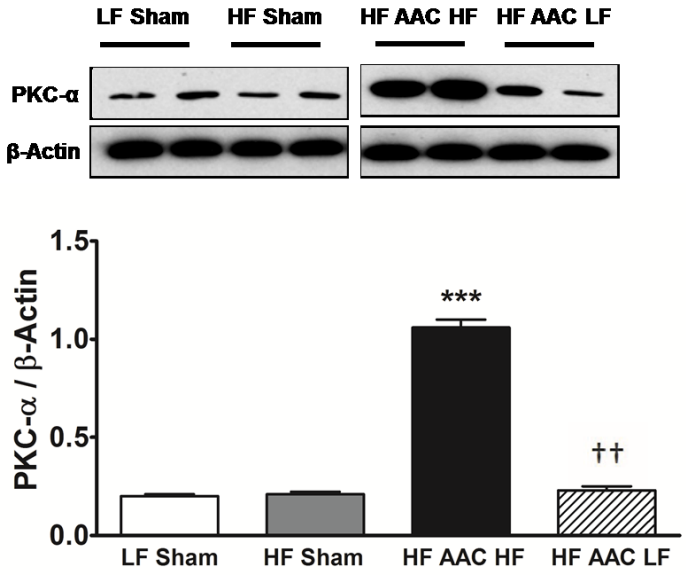
LF Sham
HF Sham
HF AAC HF
HF AAC LF
PKC-α
β-Actin
PKC-α / β-Actin
1.5
1.0
0.5
0.0
***
††
LF Sham
HF Sham
HF AAC HF
HF AAC LF

B

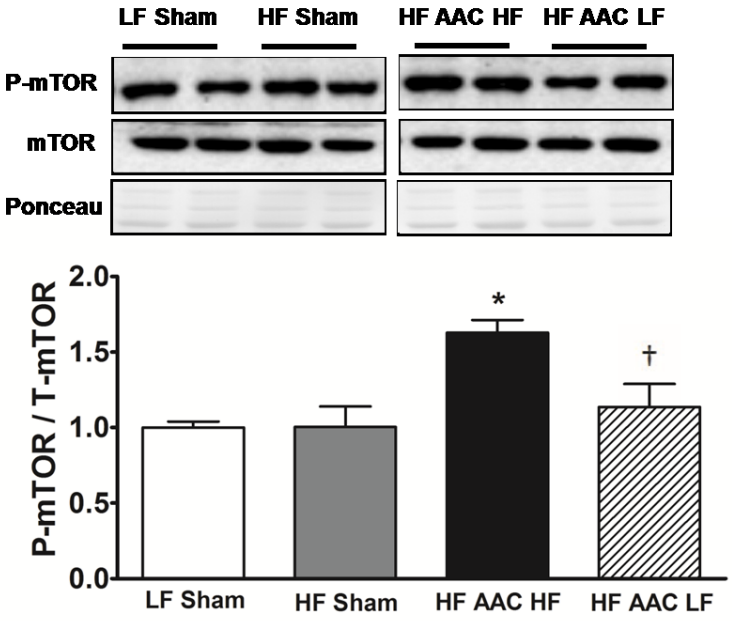
LF Sham
HF Sham
HF AAC HF
HF AAC LF
P-mTOR
mTOR
Ponceau
P-mTOR / T-mTOR
2.0
1.5
1.0
0.5
0.0
*
†
LF Sham
HF Sham
HF AAC HF
HF AAC LF

Figure 5-4

C

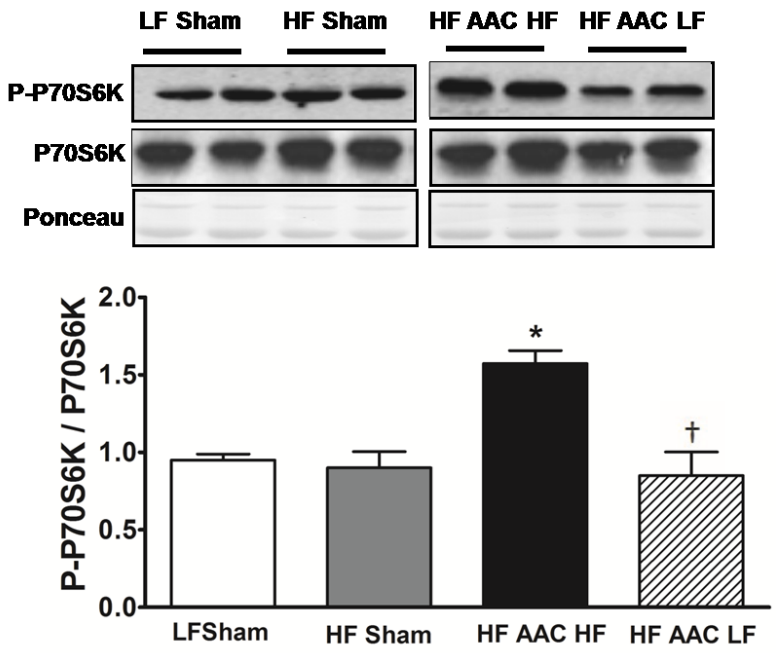
LF Sham
HF Sham
HF AAC HF
HF AAC LF
P-P70S6K
P70S6K
Ponceau
P-P70S6K / P70S6K
2.0
1.5
1.0
0.5
0.0
*
†
LFSham
HF Sham
HF AAC HF
HF AAC LF

D

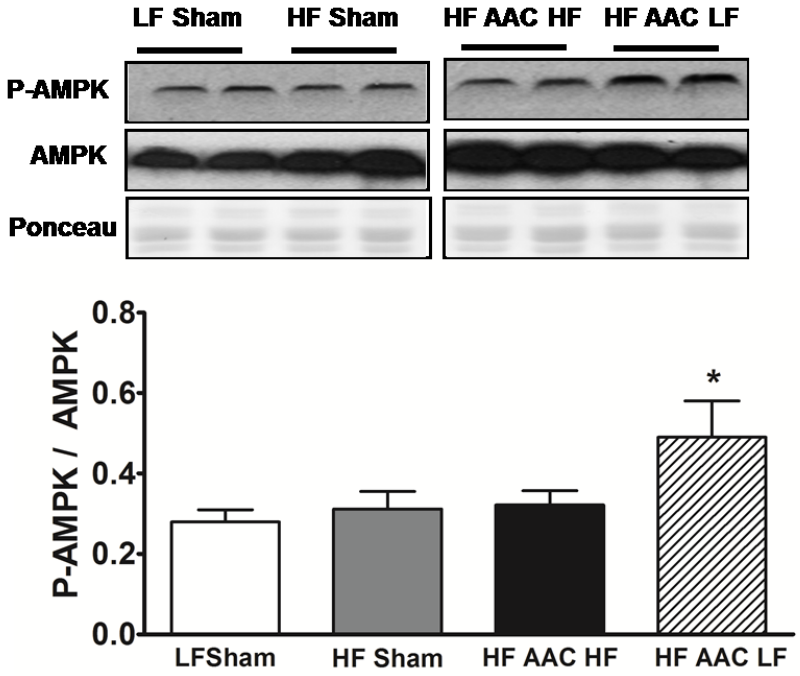
LF Sham
HF Sham
HF AAC HF
HF AAC LF
P-AMPK
AMPK
Ponceau
P-AMPK / AMPK
0.8
0.6
0.4
0.2
0.0
*
LFSham
HF Sham
HF AAC HF
HF AAC LF

Figure 5-4

Figure 5-5: Cardiac energy metabolism in LFD and HFD fed mice.

A) Insulin stimulated glucose oxidation is increased in the LFD fed sham mice. This response is markedly blunted in the HF AAC HF mice. Switching obese-heart failure mice to LFD results in a dramatic improvement in glucose oxidation. **B)** Insulin induced decrease in palmitate oxidation is blunted in the HF AAC HF mice. Switching to LFD normalizes this effect.

* $P<0.05$, ** $P<0.01$ vs. respective group W/O insulin; †† $P<0.01$ vs. HF AAC HF W/ Insulin. Values represent mean ± SEM (n=6).

A

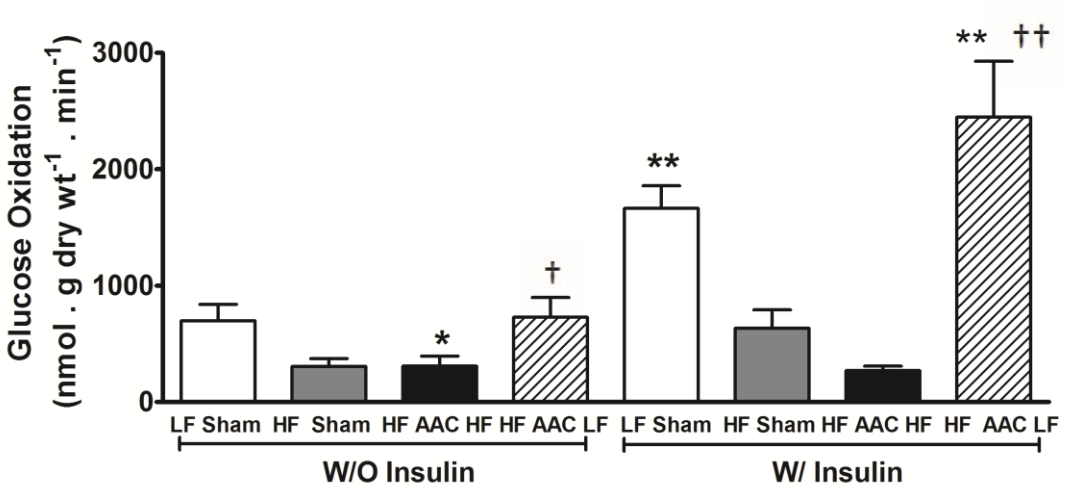
Glucose Oxidation
(nmol . g dry wt-1 . min-1)
3000
2000
1000
0
*
†
**
** ††
LF Sham HF Sham HF AAC HF HF AAC LF
LF Sham HF Sham HF AAC HF HF AAC LF
W/O Insulin
W/ Insulin

B

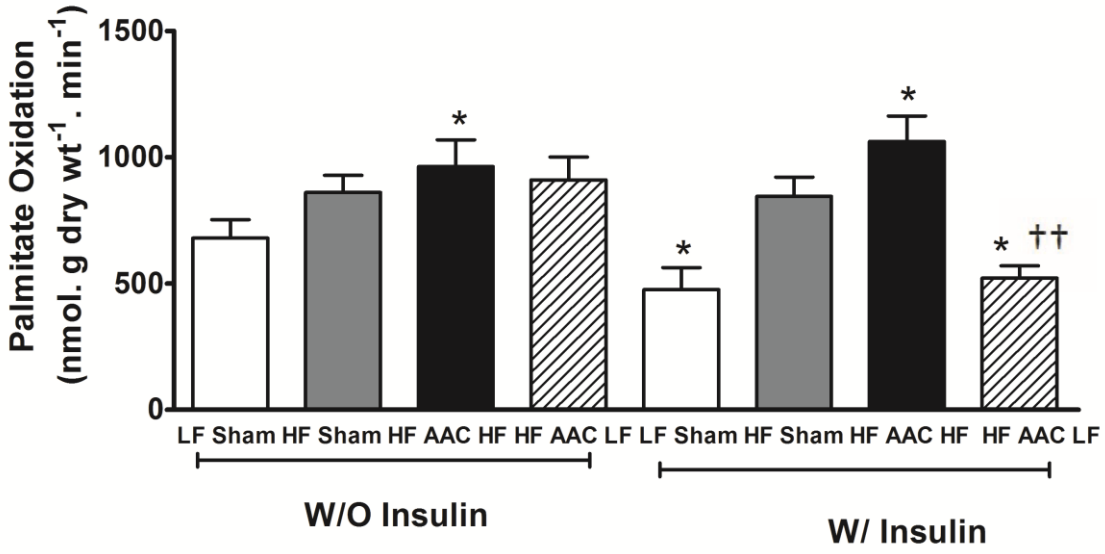
Palmitate Oxidation
(nmol. g dry wt-1 . min-1)
1500
1000
500
0
*
*
*
* ††
LF Sham HF Sham HF AAC HF HF AAC LF
LF Sham HF Sham HF AAC HF HF AAC LF
W/O Insulin
W/ Insulin

Figure 5-5

Figure 5-6: Level of LCAD acetylation and activity in hearts from LFD and HFD fed mice.

A) HFD increases expression of the acetyl transferase GCN5L1. Switching to LFD reverses this effect. **B)** No change in expression of the deacetylase SIRT3 was observed. **C)** Acetylation of LCAD is increased in response to HFD. A further increase is noted in HF AAC HF mice. Switching to LFD completely reverses this effect. **D)** LCAD activity parallels acetylation status of LCAD. **E)** LFD fed sham and HF AAC LF mice that have a lower abundance of acetylated LCAD have lower palmitate oxidation rates. The HFD fed sham and HF AAC HF mice with higher palmitate oxidation rates have higher abundance of acetylated LCAD.

*P<0.05, **P<0.01 vs. LF Sham; † P<0.05 vs. HF AAC HF; ‡ P<0.05 vs. HF Sham; Values represent mean ± SEM (n=6).

A

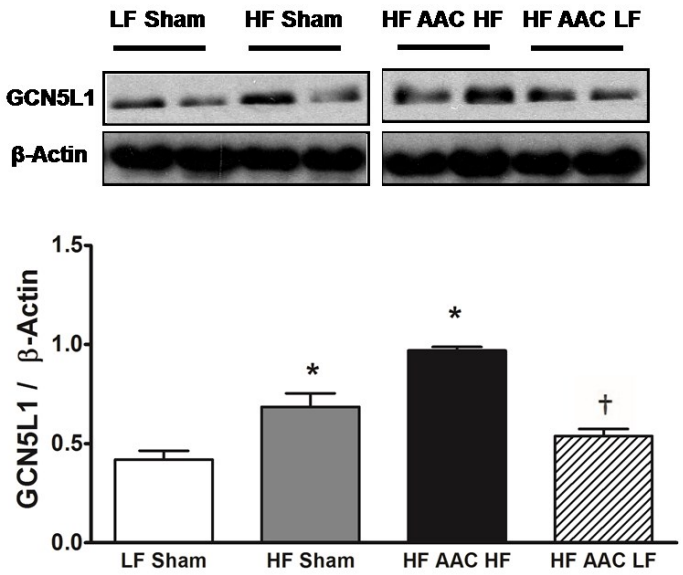
LF Sham
HF Sham
HF AAC HF
HF AAC LF
GCN5L1
β-Actin
GCN5L1 / β-Actin
1.5
1.0
0.5
0.0
*
*
†
LF Sham
HF Sham
HF AAC HF
HF AAC LF

B

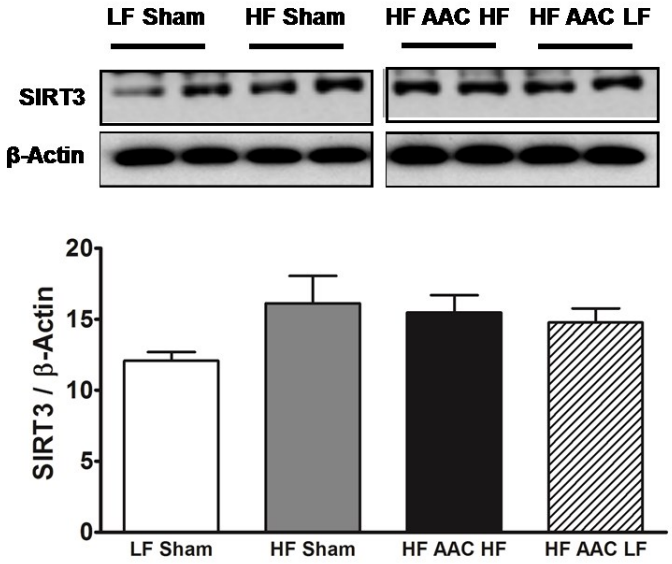
LF Sham
HF Sham
HF AAC HF
HF AAC LF
SIRT3
β-Actin
SIRT3 / β-Actin
20
15
10
5
0
LF Sham
HF Sham
HF AAC HF
HF AAC LF

Figure 5-6

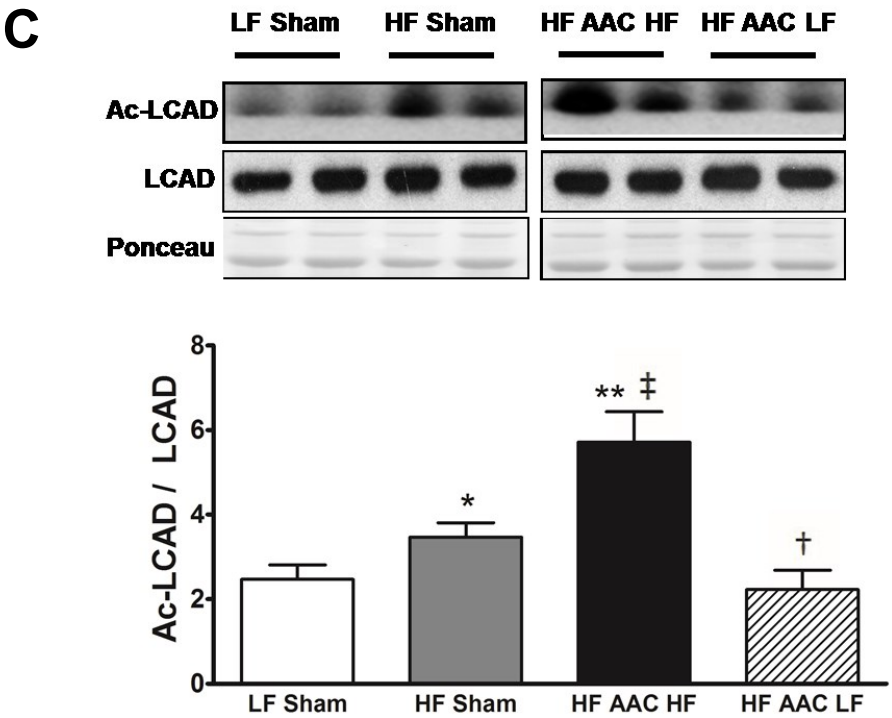
C
LF Sham
HF Sham
HF AAC HF
HF AAC LF
Ac-LCAD
LCAD
Ponceau
Ac-LCAD / LCAD
8
6
4
2
0
*
** ‡
†
LF Sham
HF Sham
HF AAC HF
HF AAC LF

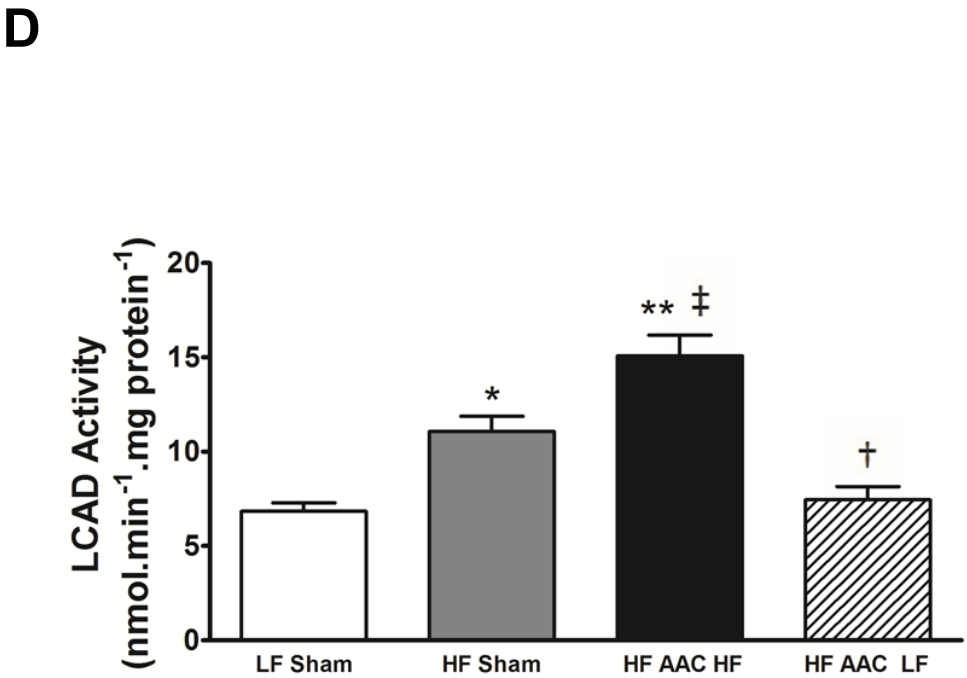
D
LCAD Activity
(nmol.min-1.mg protein-1)
20
15
10
5
0
*
** ‡
†
LF Sham
HF Sham
HF AAC HF
HF AAC LF

Figure 5-6

E

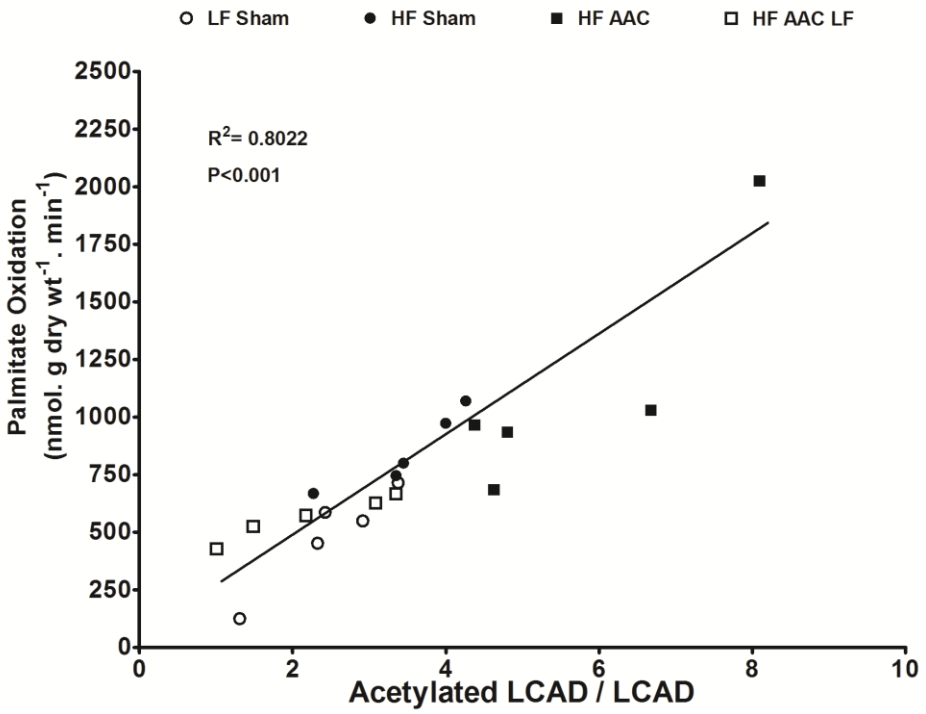
LF Sham
HF Sham
HF AAC
HF AAC LF
R2= 0.8022
P<0.001
Palmitate Oxidation
(nmol. g dry wt-1. min-1)
2500
2250
2000
1750
1500
1250
1000
750
500
250
0
0
2
4
6
8
10
Acetylated LCAD / LCAD

Figure 5-6

Figure 5-7: Insulin signaling pathway in mice fed a low or high fat diet.

A) Phosphorylation of Akt (P-Akt) is significantly increased in HF AAC LF. **B)** Phosphorylation of GSK3β is decreased by high fat feeding (HF Sham and HF AAC HF). Switching to low fat diet rescues this effect.

*$P<0.05$; $^{‡}P<0.05$ vs. HF AAC HF. Values represent mean ± SEM (n=6).

A

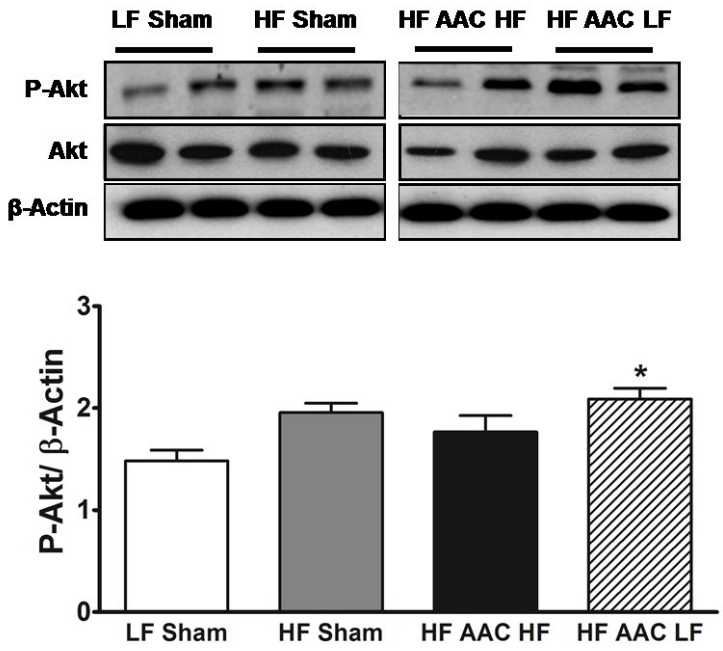
LF Sham
HF Sham
HF AAC HF
HF AAC LF
P-Akt
Akt
β-Actin
P-Akt/ β-Actin
3
2
1
0
*
LF Sham
HF Sham
HF AAC HF
HF AAC LF

B

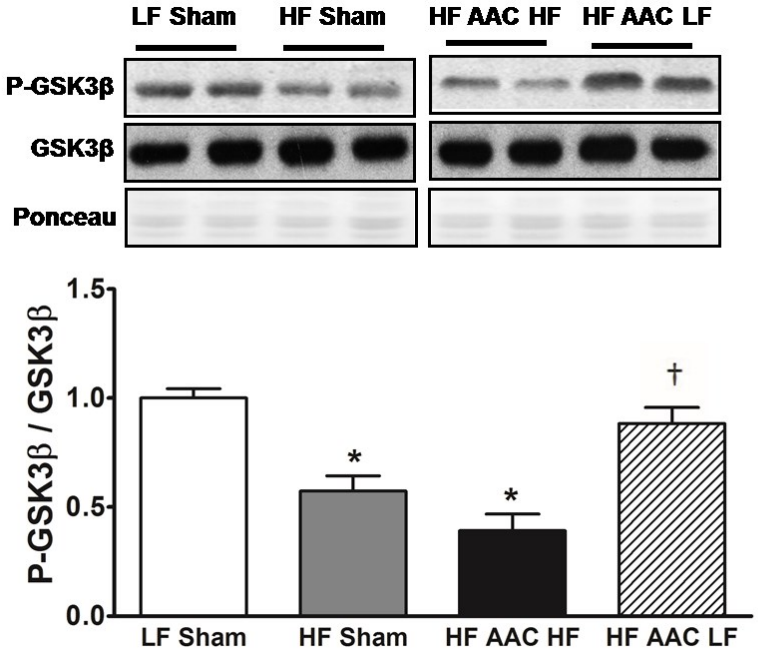
LF Sham
HF Sham
HF AAC HF
HF AAC LF
P-GSK3β
GSK3β
Ponceau
P-GSK3β / GSK3β
1.5
1.0
0.5
0.0
*
*
†
LF Sham
HF Sham
HF AAC HF
HF AAC LF

Figure 5-7

5.4 DISCUSSION

In this study we showed that obese mice with heart failure that were switched to LFD had improved cardiac function. This was accompanied by a dramatic improvement in insulin sensitivity that led to an increase in insulin-stimulated glucose oxidation and a decrease in cardiac hypertrophy. In our study, we show that by switching the obese heart failure mice to LFD, we completely reversed cardiac insulin resistance. Hearts from HF AAC HF mice developed insulin resistance that resulted in low glucose oxidation rates. On the other hand, switching these mice to LFD resulted in improved insulin sensitivity and increased glucose oxidation. Thus insulin resistance observed in HF AAC HF hearts was associated with impaired insulin signaling (Akt and GSK3b phosphorylation) and therefore decreased glucose oxidation rates.

Recent studies from our group have shown a decrease in glucose oxidation in TAC (138) and angiotensin – II (59,264) induced mouse models of heart failure. We also showed that in mice lacking malonyl CoA decarboxylase *MCD*$^{-/-}$, the enzyme that inhibits fatty acid β-oxidation through modulating malonyl CoA levels, a robust increase in cardiac insulin stimulated glucose oxidation was seen in mice on a HFD (88). Therefore, a decrease in glucose oxidation and an increase in fatty acid β-oxidation could have contributed to cardiac dysfunction in the HF AAC HF mice. In contrast, *CPT-1b*$^{+/-}$ mice that partially lack CPT-1 have decreased

cardiac fatty acid β-oxidation and they develop cardiac dysfunction and hypertrophy under mild pressure overload conditions (16). Furthermore, preserved cardiac function and attenuated cardiac hypertrophy was observed in *ACC2*$^{-/-}$ subjected to TAC when compared to WT mice subjected to TAC (136). These studies underscore the role of fatty acid β-oxidation in maintaining cardiac function in heart failure.

One effect of insulin resistance is increased fatty acid utilization by hearts. We observed increased fatty acid β-oxidation rates in hearts from obese mice with diastolic dysfunction. Switching these mice to low fat diet resulted in marked increase in glucose oxidation and a reciprocal decrease in fatty acid β-oxidation. Consistent with our results, hearts from mice fed high fat diet (61) or from ob/ob and db/db mice (58) have increased fatty acid β-oxidation. We therefore wanted to understand mechanisms that underlie dramatic changes in substrate utilization.

Several studies have shown that acetylation of lysine residues regulate activity of enzymes involved in energy metabolism (159,191,194,200). We therefore wanted to assess the acetylation status of a key enzyme in fatty acid β-oxidation, LCAD. Acetylation of LCAD was increased in obese mice with heart failure. This was associated with an increase in fatty acid β-oxidation rates in aerobically perfused hearts. In hearts from HF AAC LF mice acetylation of LCAD was decreased and so was fatty acid β-oxidation rate. Hyperacetylation of LCAD was also associated with increased LCAD activity. There is a controversy in the

literature whether acetylation of LCAD or other fatty acid β-oxidation enzymes is activating or inhibitory. Hirschey *et al* demonstrated that in hepatocytes, deacetylation of the fatty acid β-oxidative enzyme LCAD increases fatty acid β-oxidation rates (200). On the otherhand, Zhao *et al* showed that in cardiomyocytes, hyperacetylation of β-HAD, another enzyme involved in fatty acid β-oxidation resulted in its activation (159). A recent study reported increased fatty acid β-oxidation in skeletal muscle of SIRT3 KO mice (201). Consistent with the latter studies, we observed a positive correlation between acetylation of LCAD and fatty acid β-oxidation rates supporting evidence in the literature that acetylation of LCAD activates fatty acid β-oxidation.

Cardiac hypertrophy in HF AAC HF mice was estimated by increased LV mass, and increased posterior wall thickness, findings that were confirmed by *ex vivo* measurement of LV mass / tibia length. HF AAC HF mice had cardiac hypertrophy that progressed to heart failure. Mice switched to LFD continued to hypertrophy albeit to a lesser extent ultimately resulting in a lower LV mass. We therefore wanted to understand mechanisms of cardiac hypertrophy in HF AAC HF hearts. Inhibition of FoxO1 and the decrease in downstream atrogin expression have been implicated in high fat diet induced cardiac hypertrophy (265). On the otherhand, activation of FoxO1 has been shown to promote cardiac (266) and skeletal muscle atrophy (267). In several tissues, FoxO1 and 3 are known to be regulated by SIRT1 (187,188). De-acetylation of

FoxO1 by SIRT1 has been shown to repress its activity (187,188). Because FoxO1 that regulates atrophy are in turn regulated by SIRT1, we wanted to understand if SIRT1 would be involved in regulating cardiac hypertrophy in diastolic dysfunction. We observed significantly increased SIRT1 expression in HF AAC HF mice that was associated with decreased acetylation and inhibition of FoxO1 which resulted in decreased atrogin-1 expression. Atrogin-1 is associated with skeletal muscle atrophy and therefore decreases in atrogin-1 possibly contributed to cardiac hypertrophy as well. Consistent with our study, SIRT1 has been shown to be involved in the inhibition of FoxO1 (187,188) and cardiac hypertrophy (164). In HF AAC HF mice switched to low fat diet, a decrease in SIRT1 was associated with increased acetylation and activation of FoxO1 and the subsequent increase in atrogin-1 expression. In contrast, activation of FoxO1 has been shown to be involved in high fat diet induced cardiac hypertrophy and metabolic alterations. We find that a decrease in SIRT1 in HFD fed sham mice resulted in increased acetylation and therefore activation of FoxO1 leading to increase in LV mass/tibia length. Thus, cardiac hypertrophy in sham and AAC mice could involve divergent pathways.

Another pathway involved in cardiac hypertrophy is protein kinase C (PKC). PKC activity is increased during the development of heart failure (268). In a pressure overload induced model of heart failure in guinea pigs, constriction of the descending thoracic aorta was accompanied by

increase in PKC α expression during decompensated cardiac hypertrophy (269). Moreover, PKC is also involved in cardiac hypertrophy. PKC is hypothesized to modulate cardiac hypertrophy by phosphorylation of transcription factors controlling expression of hypertrophic genes. Among these transcription factors found to be modulated by PKC in agonist stimulated cardiomyocytes are c-jun and fos (270). PKC also promotes phosphorylation of mTOR and P70S6K resulting in activation of the cardiac hypertrophic pathways (271). Cardiac hypertrophy was associated with activation of mTOR and P70S6K in HF AAC HF hearts. On the other hand, in HF AAC LF hearts activation of AMPK resulted in inhibition of mTOR and P70S6K pathway that led to lesser degree of cardiac hypertrophy. In a transverse aortic constriction induced rat model of cardiac hypertrophy, AICAR, an AMPK activator reduced cardiac hypertrophy (272). Resveratrol, an AMPK activator also reduced cardiac hypertrophy in the spontaneously hypertensive rats (272). We observed an increased activation of AMPK in obese heart failure mice switched to LFD. Activation of AMPK can further activate P38MAPK (272) that can increase atrogin-1 independent of FoxO (273,275). Thus, SIRT1 mediated hypertrophy in HF AAC HF mice, while activation of AMPK and FoxO1 blunted the hypertrophic response in HF AAC LF mice. However, further studies are needed to ascertain the mechanism of cardiac hypertrophy to a lesser extent in HF AAC LF mice.

Switching HF AAC mice to low fat diet resulted in an improvement in diastolic function that was associated with a lesser degree of hypertrophy and an increase in insulin-stimulated glucose oxidation. At 8 weeks (4 weeks post-AAC) when the HF AAC mice were switched to a LFD, decompensation had already set in despite cardiac hypertrophy. Our data shows that in the HF AAC LF mice, despite continued hypertrophy (possibly due to constant AAC mediated pressure overload) an increase in insulin-stimulated glucose oxidation is able to improve both diastolic and systolic function. This study clearly demonstrates the importance of targeting cardiac energy metabolism in the treatment of hypertrophy associated heart failure.